JOC Article

Highly Coupled Dyads Based on Phthalocyanine−Ruthenium(II) Tris(bipyridine) Complexes. Synthesis and Photoinduced Processes

Ana González-Cabello,[†] Purificación Vázquez,*[,†] Tomás Torres,*[,†] and Dirk M. Guldi*[,‡]

Departamento de Química Orgánica (C-I), Facultad de Ciencias, Universidad Autónoma de Madrid, Cantoblanco, 28049-Madrid, Spain, and Radiation Laboratory, University of Notre Dame, South Bend, Indiana, 46556

tomas.torres@uam.es; guldi.1@nd.edu

Received February 13, 2003

A new series of multicomponent ZnPc−Ru(bpy)$_3$ systems, **1a**−**c**, consisting of a zinc-phthalocyanine linked through conjugated and/or nonconjugated connections to a ruthenium(II) tris(bipyridine) complex, has been synthesized. The ruthenium complexes **1a**−**c** were prepared from phthalocyanines **2a**−**c**, bearing a 4-substituted-2,2′-bipyridine ligand by treatment with [Ru(bpy)$_2$Cl$_2$]·2H$_2$O. Different synthetic strategies have been devised to prepare the corresponding dyad precursors (**2a**−**c**). Compound **2a**, for example, with an ethenyl bridge, was synthesized by statistical condensation of 4-*tert*-butylphthalonitrile and 5-[(*E*)-2-(3,4-dicyanophenyl)ethenyl]-2,2′-bipyridine (**3**) in the presence of zinc chloride. Compounds **2b** and **2c**, having, respectively, an amide or an ethynyl bridge, were prepared following a different synthetic approach. The method involves the coupling of an appropriate 5-substituted-2,2′-bipyridine to an unsymmetrical phthalocyanine suitably functionalized with an amino (**4**) or an ethynyl group (**5**). The photophysical properties of the dyads that are ZnPc−Ru(bpy)$_3$ **1a**−**c** and related model compounds have been determined by a variety of steady-state (i.e., fluorescence) and time-resolved methods (i.e., fluorescence and transient absorption). Clearly, intramolecular electronic interactions between the two subunits dominate the photophysical events following the initial excitation of either chromophore. These intramolecular interactions lead, in the case of photoexcited ZnPc, to faster intersystem crossing kinetics compared to a **ZnPc** reference, while photoexcited [Ru(bpy)$_3$]$^{2+}$ undergoes a rapid and efficient transduction of triplet excited-state energy to the Pc.

Introduction

Many photoactive molecular architectures, such as dyads, triads, and higher order arrays, have been designed and studied in recent years as model systems to process efficiently solar energy and, thereby, replicate the natural analogue.[1] Upon selective light illumination of a given chromophore, such multicomponent model systems are able to undergo directional electron and/or energy transfer. Among the many chromophores used, porphyrin and ruthenium(II) polypyridine complexes hold great promise on account of their increased absorptive cross sections at those wavelengths corresponding to maxima of emission in the solar spectrum.

Furthermore, they have exerted noteworthy impact as components in integrated molecular arrays, both for the mimicry of processes taking place in nature and for the development of devices at the molecular level.[2] Successful strategies for attaching the different subunits impose the use of either covalent[3] or noncovalent[4] bonds.

In these systems, the extent of electronic communication, both in the ground state and in the excited state,

* To whom correspondence should be addressed. Phone: (+34) 91 3974151. Fax: (+34) 91 3973966 (T.T.; P.V.).
[†] Universidad Autónoma de Madrid.
[‡] University of Notre Dame.

(1) (a) Balzani, V.; Scandola, F. In *Supramolecular Photochemistry*; Kemp, T. J., Ed.; Ellis Horwood: London, 1991. (b) Wasielewski, M. R. *Chem. Rev.* **1992**, *92*, 435. (c) Kurreck, H.; Huber, M. *Angew. Chem., Int. Ed. Engl.* **1995**, *34*, 849. (d) Harriman, A.; Ziesssel, R. *Chem. Soc. Rev.* **1996**, 41. (e) Lynke, M.; Chambron, J.-C.; Heitz, V.; Sauvage, J.-P. *J. Am. Chem. Soc.* **1997**, *119*, 11329. (f) Chambron, J.-C.; Collin, J.-P.; Dalbavie, J.-O.; Dietrich-Buchecker, C. O.; Heitz, V.; Odobel, F.; Solladié, N.; Sauvage, J.-P. *Coord. Chem. Rev.* **1998**, *178*−*180*, 1299. (g) Flamigni, L.; Barigelletti, F.; Armaroli, N.; Collin, J.-P.; Sauvage, J.-P.; Gareth Williams, J. A. *Chem. Eur. J.* **1998**, *4*, 1744. (h) Collin, J.-P.; Gaviña, P.; Heitz, V.; Sauvage, J.-P. *Eur. J. Inorg. Chem.* **1998**, 1. (i) Flamigni, L.; Barigelletti, F.; Armaroli, N.; Ventura, B.; Collin, J.-P.; Sauvage, J.-P.; Gareth-Williams, J. A. *Inorg. Chem.* **1999**, *38*, 661. (j) Allwood, J. L.; Burrell, A. K.; Officer, D. L.; Scott, S. M.; Wild, K. Y.; Gordon, K. C. *Chem. Commun.* **2000**, 747. (k) Schild, V.; Van Loyen, D.; Duerr, H.; Bouas-Laurent, H.; Turro, C.; Woerner, M.; Pokhrel, M. R.; Bossmann, S. H. *J. Phys. Chem. A* **2002**, *106*, 9149. (l) Guldi, D. M.; Luo, C.; Swartz, A.; Gomez, R.; Segura, J. L.; Martín, N.; Brabec, C.; Sariciftci, N. S. *J. Org. Chem.* **2002**, *67*, 1141.

(2) (a) Sessler, J. L.; Capuano, V. L.; Burrell, A. K. *Inorg. Chim. Acta* **1993**, *204*, 93. (b) Hamachi, I.; Tanaka, S.; Shinkai, S. *J. Am. Chem. Soc.* **1993**, *115*, 10458. (c) LeGourriérec, D.; Anderson, M.; Davidson, J.; Mukhtar, E.; Sun, L.; Hammarström, L. *J. Phys. Chem. A* **1999**, *103*, 557. (d) Hamachi, I.; Tsukiji, S.; Shinkai, S.; Oishi, S. *J. Am. Chem. Soc.* **1999**, *121*, 5500. (e) Hamachi, I.; Shinkai, S. *Eur. J. Org. Chem.* **1999**, 539. (f) Lintuoto, J. M.; Borovkov, V. V.; Inoue, Y. *Tetrahedron Lett.* **2000**, *41*, 4781. (g) Hu, Y.-Z.; Tsukiji, S.; Shinkai, S.; Oishi, S.; Hamachi, I. *J. Am. Chem. Soc.* **2000**, *122*, 241. (h) Serroni, S.; Campagna, S.; Puntoriero, F.; Juris, A.; Denti, G.; Balzani, V.; Venturi, M.; Janzen, D.; Mann, K. R. *Inorg. Synth.* **2002**, *33*, 10.

(3) Harriman, A.; Ziessel, R. *Coord. Chem. Rev.* **1998**, *171*, 331.

10.1021/jo0341968 CCC: $25.00
Published on Web 10/07/2003

between the individual components is largely dependent upon the nature of the bridge, which connects the two interacting centers. The role played by the different spacer is also structural, since its chemical nature determines the flexibility or rigidity of the system. It is essential that the multicomponent system is rigid, so as to ensure good geometrical control and favor long-lived charge-separated states. Consequently, the choice of the bridge that connects the photoactive subunits becomes of central importance. The connector must also be sufficiently versatile to enable construction of different (with respect to the size, shape, composition, and organization) supermolecules.

On the other hand, phthalocyanines (Pcs)[5,6] are porphyrin analogues that exhibit a number of unique electronic properties (derived from their two-dimensional highly delocalized 18-π-electron system)[5] that render them interesting candidates to be linked to ruthenium(II) polypyridine complexes for the study of energy and/or electronic transfer processes. Our interest has centered on phthalocyanines and related compounds, since they are exceptionally stable toward heat/light and exhibit intense absorption in the 600−700 nm region of the visible spectrum.

To the best of our knowledge, very few examples of phthalocyanines linked to a ruthenium(II) polypyridine system have been described.[7] Herein we describe the synthesis and the photophysical properties of a new series of ZnPc−ruthenium(II) trisbipyridine systems ZnPc−$Ru(bpy)_3$ **1a**−**c** to fine tune the electronic coupling between ZnPc and $[Ru(bpy)_3]^{2+}$.

Results and Discussion

Synthesis. Our synthetic approach toward phthalocyanine−$Ru(bpy)_3$ dyads (**1a**−**c**) relies upon the reaction between a ruthenium precursor complex, $[Ru(bpy)_2Cl_2]\cdot 2H_2O$, and the corresponding unsymmetrical phthalocyaninatozinc(II) (**2a**−**c**) bearing a 4-substituted-2,2′-bipyridine subunit (Scheme 1).

SCHEME 1

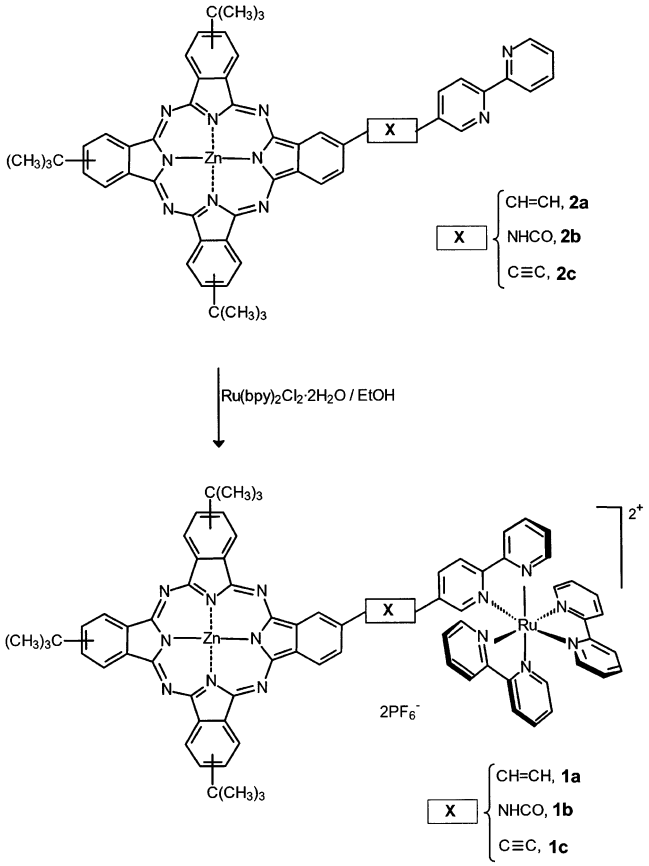

SCHEME 2

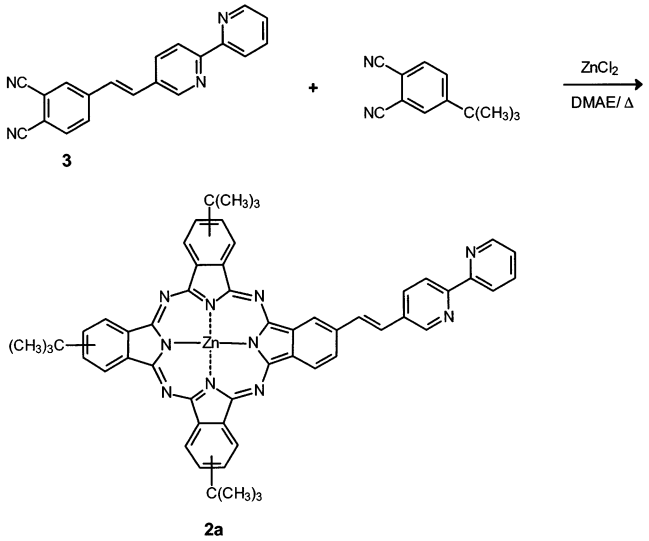

Two different pathways were developed for the synthesis of the unsymmetrical phthalocyaninato compounds **2a**−**c**, depending on the spacer that connects the phthalocyanine (ZnPc) and the 2,2′-bipyridine moieties (Schemes 2 and 3).

Compound **2a**, having an ethenyl bridge, was synthesized by statistical condensation of 4-*tert*-butylphthalonitrile[8a] and 5-[(*E*)-2-(3,4-dicyanophenyl)ethenyl]-2,2′-bipyridine (**3**) (1:3 molar ratio), using *N*,*N*-dimethylaminoethanol (DMAE) as a solvent in the presence of zinc chloride (Scheme 2). Phthalonitrile **3** was prepared in

(4) (a) Lehn, J. M. *Angew. Chem., Int. Ed. Engl.* **1988**, *27*, 89. (b) Harriman, A.; Magda, D. J.; Sessler, J. L. *J. Chem. Soc., Chem. Commun*. **1991**, 345. (c) Gust, D.; Moore, T. A. *Top. Curr. Chem*. **1991**, *159*, 103. (d) Paddon-Row, M. N. *Acc. Chem. Res*. **1994**, *27*, 18. (e) Sessler, J. L.; Brown, C. T.; O'Connor, D.; Springs, S. L.; Wang, R.; Sathiosatham, M.; Hirose, T. *J. Org. Chem*. **1998**, *63*, 7370. (f) Kuroda, Y.; Sugou, K.; Sasaki, K. *J. Am. Chem. Soc.* **2000**, *122*, 7833.

(5) (a) *Phthalocyanines*: *Properties and Applications*; Leznoff, C. C.; Lever, A. B. P., Eds.; VCH: Weinheim, 1989−1996; Vols. 1−4. (b) Hanack, M.; Heckmann, H.; Polley, R. In *Methods in Organic Chemistry* (*Houben-Weyl*); Schaumann, E. Ed.; Georg Thieme Verlag: Stuttgart, 1998; Vol. E 9d, pp 717−833. (c) De la Torre, G.; Nicolau, M.; Torres, T. In *Supramolecular Photosensitive and Electroactive Materials*; Nalwa, H. Ed.; Academic Press: New York, 2001; pp 1−111. (d) Rodríguez-Morgade, M. S.; De la Torre, G.; Torres T. In *Porphyrin Handbook*, Kadish, K. M., Smith, K. M., Guilard, R., Eds.; Academic Press: New York, 2003; Vol. 15, ch 99.

(6) For recent papers of our group in this field, see: (a) Keller, U.; Del Rey, B.; Rojo, G.; Agulló-López, F.; Nonell, S.; Martí, C.; Brasselet, S.; Ledoux, I.; Zyss, J.; Torres, T. *J. Am. Chem. Soc.* **1998**, *120*, 12808. (b) Maya, E. M.; Vázquez, P.; Torres, T. *Chem. Eur. J*. **1999**, *5*, 2004. (c) Gouloumis, A.; Liu, S.-G.; Sastre, Á.; Vázquez, P.; Echegoyen, L.; Torres, T. *Chem. Eur. J*. **2000**, *6*, 3600. (d) De la Torre, G.; Gouloumis, A.; Vázquez, P.; Torres, T. *Angew. Chem., Int. Ed. Engl*. **2001**, *40*, 2895. (e) Claessens, C. G.; González-Rodríguez, D.; Torres, T. *Chem. Rev*. **2002**, *102*, 835. (f) Claessens, C. G.; Torres, T. *Angew. Chem., Int. Ed. Engl*. **2002**, *41*, 2561. (g) Claessens, C. G.; Torres, T. *J. Am. Chem. Soc*. **2002**, *124*, 14522.

(7) Kimura, M.; Hamakawa, T.; Muto, T.; Hanabusa, K.; Shirai, H.; Kobayashi, N.; *Tetrahedron Lett*. **1998**, *39*, 8471.

SCHEME 3

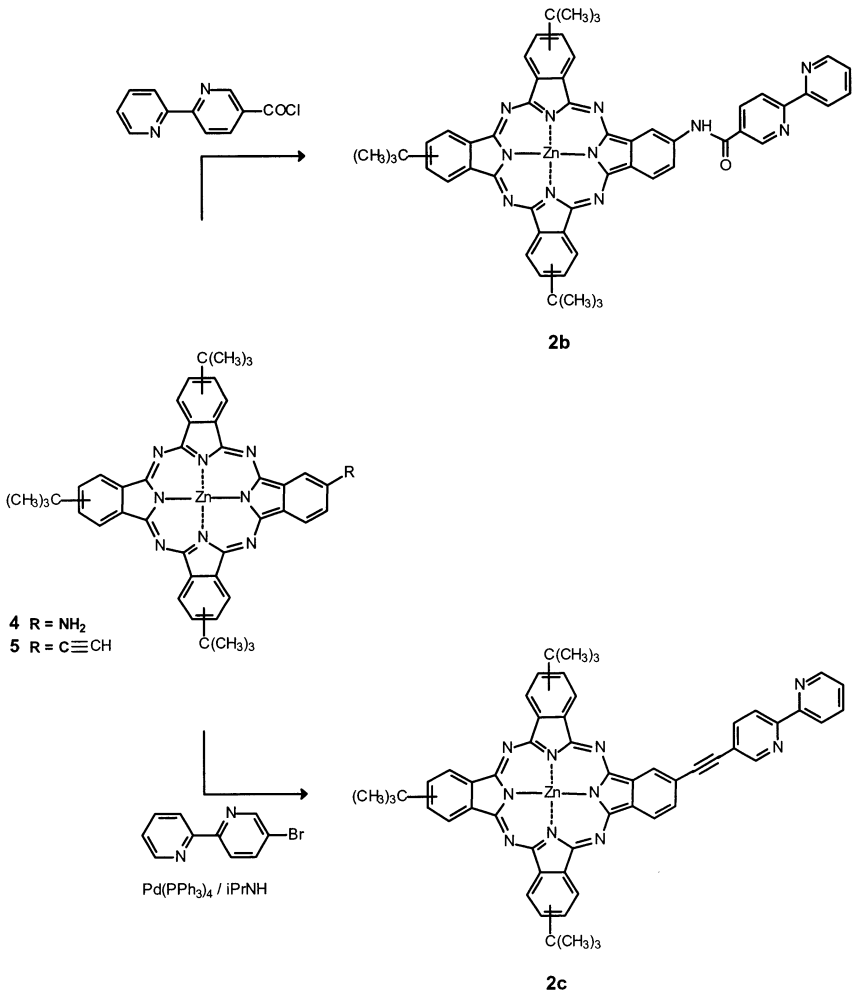

72% yield by refluxing 1,2-dicyano-4-benzylphosphonate[8b] and 5-formyl-2,2′-bipyridine in a low basic aqueous heterogeneous medium and in the absence of organic solvents. A central requirement is the *trans* geometry in the double bond, since better electronic delocalization is expected for this configuration. The ^{1}H NMR coupling constant with J (H, H) values of 16.5 Hz confirmed the *trans* geometry.

Compounds **2b** and **2c**, having, respectively, an amide or an ethynyl bridge, were prepared following a different synthetic approach. The method involves the coupling of an appropriate 5-substituted-2,2′-bipyridine to an unsymmetrical phthalocyanine, which is suitably functionalized with an amino **4** or, alternatively, with an ethynyl group **5** (Scheme 3). The preparation of the unsymmetrical phthalocyanine that carries a terminal ethynyl group **5** was carried out following a synthetic procedure previously described.[6b] The synthesis of the unsymmetrical phthalocyaninato **4** bearing an amino group was performed by a mixed condensation of the 4-*tert*-butylphthalonitrile (3 equiv) and 4-aminophthalonitrile[9] in the presence of zinc chloride.

The synthesis of compound **2b** was carried out by coupling 5-chlorocarbonyl-2,2′-bipyridine[10] to aminotri-*tert*-butylphthalocyaninatozinc(II) (**4**) in *N*,*N*-dimethylacetamide, affording compound **2b** in moderate yields after chromatographic purification (Scheme 3). This compound **2b** was previously prepared by reduction of nitrotri-*tert*-butylphthalocyaninatozinc(II).[11]

Phthalocyaninato **2c** was prepared by a palladium(0)-promoted cross-coupling reaction between 5-bromo-2,2′-bipyridine[12] and ethynyltri-*tert*-phthalocyaninatozinc(II)[6b] (**5**) in freshly distilled and deaerated diisopropylamine as a base (Scheme 3). Since compound **2c** was contaminated by a small amount of the corresponding homocoupled dimer of **5**, separation by flash chromatography rendered necessary.

Compounds **2a**−**c** are only slightly soluble in $CDCl_3$ and were characterized by FTIR, UV−vis spectroscopy, mass spectrometry (liquid secondary ion mass spectrometry (LSIMS)), and elemental analysis (see Experimental

(8) Larner, B. W.; Peters, A. T. *J. Chem. Soc.* **1952**, 680. (b) Boyle, R. W.; Van Lier, J. E. *Synlett* **1993**, 351.

(9) (a) Griffiths, J.; Roozpeikar, B. *J. Chem. Soc., Perkin Trans. 1* **1976**, 42. (b) Young, J. G.; Onyebuagu, W. *J. Org. Chem.* **1990**, *55*, 2155.

(10) Martens, C. F.; Schenning, A. P. H. J.; Feiters, M. C.; Heck, J.; Beurskens, G.; Beurskens, P. T.; Steinwender, E.; Nolte, R. J. M. *Inorg. Chem.* **1993**, *32*, 3029.

(11) Kudrevich, S. V.; Ali, H.; van Lier, J. E. *J. Chem. Soc., Perkin Trans. 1* **1994**, 2767.

(12) (a) Barton, D. H. R.; Crich, D.; Mortherwell, W. B. *Tetrahedron Lett.* **1983**, *45*, 4979. (b) Barton, D. H. R.; Lacher, B.; Zard, S. Z. *Tetrahedron* **1987**, *43*, 4321. (c) Romero, F. M.; Ziessel R. *Tetrahedron Lett.* **1995**, *36*, 6471.

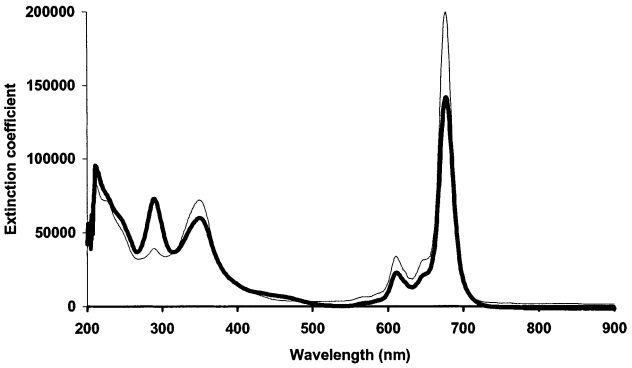

FIGURE 1. Electronic spectra in THF of **1b** (4.8×10^{-6} M) (solid line) and **2b** (4.2×10^{-6} M) (thin line).

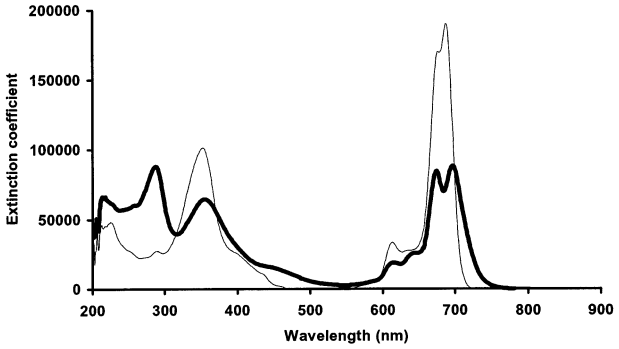

FIGURE 2. Electronic spectra in THF of **1a** (8.59×10^{-6} M) (solid line) and **2a** (3.24×10^{-6} M) (thin line).

Section). ^{1}H NMR spectra are uninformative (mixture of regioisomers).

The ruthenium complexes of the unsymmetrical phthalocyanines **2a**−**c** were prepared according to a described procedure.[13]

Dyads **1a**−**c** were synthesized by refluxing [Ru(bpy)$_2$Cl$_2$]·2H$_2$O and the corresponding phthalocyaninato **2a**−**c** in ethanol (Scheme 1). TLC following the disappearance of **2a**−**c** monitored the reaction. After filtration, the solution was concentrated under reduced pressure and the greenish solid was washed with hot water to remove unreacted [Ru(bpy)$_2$Cl$_2$]. The solid residue was then dissolved in acetone, and an aqueous solution of NH_4PF_6 was added dropwise, producing an anionic exchange and affording compounds **1a**−**c** in 40−71% yield.

Compounds **1a**−**c** are reasonably soluble in tetrahydrofurane, benzonitrile, and acetonitrile but are insoluble in methylene chloride.

All the compounds were characterized by FTIR, UV−vis spectroscopy, mass spectrometry (MALDI-TOF), and elemental analysis (see Experimental Section).

Figures 1−3 show the UV−vis spectra in THF of ZnPc−Ru(bpy)$_3$ dyads **1a**−**c** and their precursors **2a**−**c**.

The spectrum of **1b** is quite similar to that of the parent compound **2b** (Figure 1). This conclusion emerged upon considering the absorption maximum of the Q band, which appears at 677 nm. However, there are some differences in the higher-energy region due to the absorption of the $[Ru(bpy)_3]^{2+}$ complex. This is manifested in several additional bands (i.e., at 213 and 289 nm) and the higher absorptivity of the Soret band at *ca*. 340 nm. Furthermore, it is possible to observe a shoulder around 450 nm, most probably corresponding to the metal-to-ligand charge-transfer (MLCT) band of the ruthenium complex. It can be considered that the spectrum of the dyad **1b**, with the exception of a decrease in the extinction coefficient of the Q band, is the result as a simple sum of those of $[Ru(bpy)_3]^{2+}$ and phthalocyaninato **2b**.

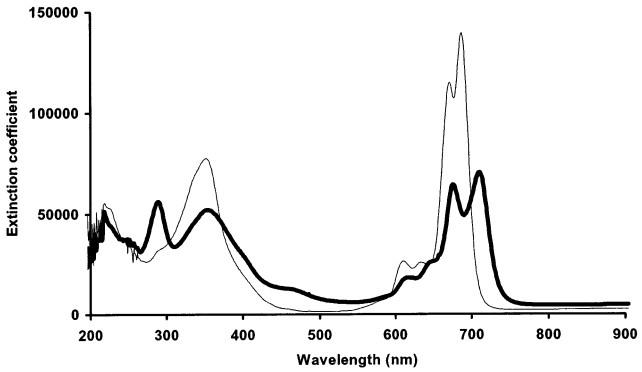

FIGURE 3. Electronic spectra in THF of **1c** (7.36×10^{-6} M) (solid line) and **2c** (5.04×10^{-6} M) (thin line).

On the contrary, in the case of the dyads **1a** and **1c**, which have conjugated ethenyl and ethynyl bridges, respectively, the Q band undergoes a remarkable broadening and splitting with regard to the parent compounds, that is, **2a** and **2c** (Figures 2 and 3). Moreover, the Q bands of dyads **1a** and **1c** are significantly red shifted (9−23 nm in tetrahydrofurane). This effect is indicative of some, although weak, interaction in the ground state between the two moieties phthalocyanine and ruthenium complex. This interaction appears stronger in the case of the ethynyl-spaced dyad, **1c**, probably due to a larger intramolecular electronic coupling between the ZnPc subunit and the ruthenium complex as compared with the ethenyl-bridged dyad.

Photophysics. Because of the amphiphilic nature of **1a**−**c**, they are only soluble in tetrahydrofurane and to a somewhat lesser extent in benzonitrile. Fewer or more polar solvents are proven inadequate to either solvate the hydrophilic $[Ru(bpy)_3]^{2+}$ moiety or the hydrophobic ZnPc one and, thus, fail to dissolve **1a**−**c**. Consequently, aggregation phenomena take place, as indicated, for example, by notable broadening of the ground-state transitions and by lower extinction coefficients, which convert the monomeric samples into clusters or aggregates of indefinite sizes.

Fluorescence Measurements. The emission properties of a tetra-*tert*-butylphthalocyanine ZnPc[14a] used as a reference can be summarized as follows: ZnPc reference fluoresces strongly at 680 nm (1.82 eV) with an overall quantum yield of 0.3. As far as the ZnPc fluorescence in complexes **1a**−**c** is concerned, the emission maxima shift parallel with the singlet ground-state transitions. Figure 4 summarizes the emission spectra of **1a**−**c** and the ZnPc reference. The following maxims were observed: 688 nm

(13) (a) Hamachi, I.; Tanaka, S.; Tsukiji, S.; Shinkai, S.; Oishi, S. *Inorg. Chem*. **1998**, *37*, 4380. (b) Hamachi, I.; Shinkai, S. *Eur. J. Org. Chem*. **1999**, 539. (c) Hissler, M.; Harriman, A.; Khatyr, A.; Ziessel, R. *Chem. Eur. J*. **1999**, *11*, 3366.

(14) (a) Commercially available tetra-*tert*-butylphthalocyanine (ZnPc) (mixture of regioisomers) was used as a reference. (b) Ruthenium(II) tris-bipyridine chloride $[Ru(bpy)_3]^{2+}$ was used as a reference.

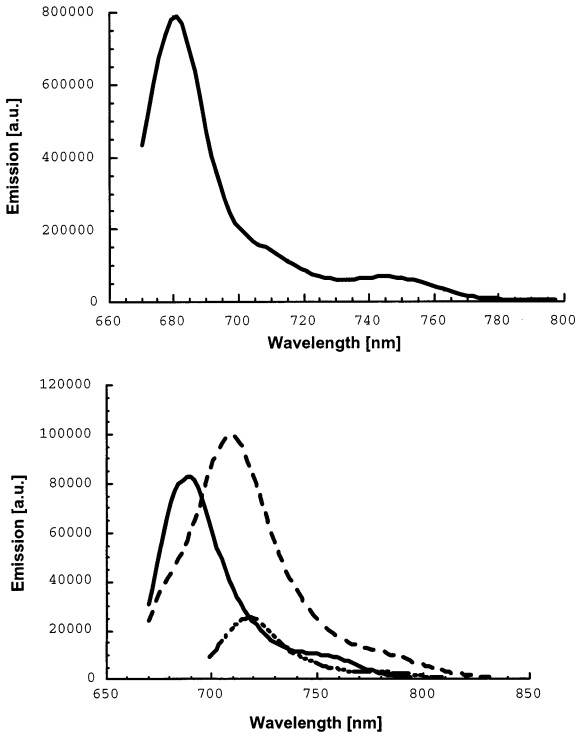

FIGURE 4. Top: Fluorescence spectra of ZnPc in THF at room temperature; 670 nm excitation wavelength. Bottom: Fluorescence spectra of **1a** (solid line), **1b** (dashed line), and **1c** (dotted line) at room temperature with matching absorption at the 650 nm excitation wavelength ($OD_{660\ nm} = 0.2$).

(**1a**), 708 nm (**1b**), 722 nm (**1c**). Again, the notably stronger coupling exhibited by the acetylene-bridged ensemble gives rise to lower energies for the radiative transition. The exact energies range between 1.80 eV (**1a**) and 1.72 eV (**1c**), relative to 1.82 eV seen for the ZnPc reference. Despite these perturbations, the underlying Stokes shifts, the energetic difference between singlet ground and singlet excited states, are surprisingly on the same order, 200 cm^{-1}. At the same time, the constant Stokes shifts put more weight on our spectral assignment.

Another observable, which in **1a**−**c** is subject to discernible changes, is the fluorescence quantum yields. Values, typically 1/10 (**1a**, 0.036; **1b**, 0.04; **1c**, 0.01) that of the ZnPc reference (0.3), indicate some acceleration of the fluorescence decay. Additionally, comparing the emission in moderately polar THF with that in strongly polar benzonitrile revealed a shift to lower energies and an extra, although moderate, amplification of the quenching (*i.e.*, a factor of ∼2). We will demonstrate below that charge separation is, however, endothermic ($-\Delta G_{CS} = -0.1$ eV; E_{red} ($[Ru(bpy)_3]^{2+}/[Ru(bpy)_3]^{+}$) = −1.3 V *versus* SCE; E_{ox} ($ZnPc/ZnPc^{\bullet+}$) = +0.6 V *vs* SCE), which leads us to erase this pathway among the possible options. A more likely scenario implies notable through-bond effects, imposed by the heavy nucleus of the ruthenium center in $[Ru(bpy)_3]^{2+}$ on the spin−orbit coupling of the ZnPc's n−*π transitions. This notion appears even more realistic, considering the complete abolishment of fluorescence in ruthenium porphyrins[15] and similar effects reported in iron porphyrins covalently linked to either zinc or metal-free porphyrins.[16]

For the emission of the $[Ru(bpy)_3]^{2+}$ moiety in **1a**−**c**, in the form of a MLCT luminescence with a maximum at 630 nm, a quantum yield of $\sim 10^{-4}$ was determined. As an internal reference value, the $[Ru(bpy)_3]^{2+}$ reference[14b] emits with an overall quantum yield of 0.04.[17] Please note that the significant overlap of the ZnPc and $[Ru(bpy)_3]^{2+}$ ground-state absorption obstructs accurate measurements, so that the given value should be only regarded as an upper limit. Regardless of this inaccuracy, the noted quenching speaks for a rapid deactivation. Again, two pathways are feasible: (i) transduction of triplet energy to the ZnPc moiety or (ii) charge separation, yielding $ZnPc^{\bullet+}-[Ru(bpy)_3]^{+}$. The energy gaps, spanning between the $[Ru(bpy)_3]^{2+}$ and ZnPc triplets (*i.e.*, 0.8 eV) relative to that for an electron transfer (*i.e.*, ∼0.2 eV), seem to speak in favor of the energy-transfer route.

Time-resolved emission measurements shed further light onto the intramolecular interactions between ZnPc and $[Ru(bpy)_3]^{2+}$ in **1a**−**c** and possible deactivation processes, as they may emerge from these interactions. In contrast to the above steady-state measurements, these experiments help to dissect the individual contribution connected to the emissive states of ZnPc (*i.e.*, singlet excited state) and $[Ru(bpy)_3]^{2+}$ (*i.e.*, triplet excited MLCT state). In particular, the ZnPc fluorescence lifetime in **1a**−**c**, as registered in the area of maximum emission, reveals a trend resembling that of the quantum yields **1b** (1.40 ns) > **1a** (1.24 ns) > **1c** (1.08 ns). However, one notable discrepancy emerges: the changes in the lifetime, relative to a ZnPc reference (3.8 ns), are substantially smaller than the changes in quantum yields (*vide infra*). This observation points unequivocally to an intrinsic property of the ZnPc moiety in **1a**−**c**, governed probably by through-bond-mediated interactions.

The emissive lifetimes of $[Ru(bpy)_3]^{2+}$ in **1a**−**c** show more dramatic effects. Relative to a value of 640 ns measured for the $[Ru(bpy)_3]^{2+}$ reference in deoxygenated acetonitrile, the lifetimes in **1a**−**c** lie between 2.9 and 6.7 ns; see Figure 5.

Transient Absorption Measurements. Excitation (18 ps) of the ZnPc reference with 355-nm laser pulses resulted in characteristic absorption changes in the spectral region between 500 and 960 nm. A net decrease of the absorption was observed in regions that are dominated by strong ZnPc ground-state transitions, for example, by the S_0-S_2 Soret band (*i.e.*, 348 nm) and S_0-S_1 Q band (*i.e.*, 614 and 680 nm). This suggests consumption of ZnPc as a result of converting the phthalocyanine singlet ground state to the corresponding singlet excited state, ^{1}*ZnPc. An immediately formed absorption in the red accompanies the bleaching associated with the singlet ground state. Both singlet excited state features, that is, transient absorption and bleaching, uniformly give rise to a singlet lifetime of 3.6 ± 0.2 ns. The fate of the singlet

(15) (a) Levine, L. M. A.; Holton, D. *J. Phys. Chem.* **1988**, *92*, 714. (b) Rillema, D. P.; Nagle, J. K.; Barringer, L. F.; Meyer, T. J. *J. Am. Chem. Soc.* **1981**, *103*, 56. (c) Rodríguez, J.; Kirmaier, C.; Holton, D. *J. Am. Chem. Soc.* **1989**, *111*, 6500.

(16) (a) Osuka, A.; Maruyama, K.; Mataga, N.; Asahi, T.; Yamazaki, I.; Tamai, N. *J. Am. Chem. Soc.* **1990**, *112*, 4958. (b) Norsten, T. B.; Chichak, K.; Branda, N. R. *Tetrahedron* **2002**, *58*, 639. (c) Kilsa, K.; Kajanus, J.; Larsson, S.; Macpherson, A. N.; Martensson, J.; Albinsson, B. *Chem. Eur. J.* **2001**, *7*, 2122.

(17) (a) Balzani, V.; Luis, A.; Venturi, M.; Campagna, S.; Serroni, S. *Chem. Rev.* **1996**, *96*, 759. (b) Dürr, H.; Bossmann, S. *Acc. Chem. Res.* **2001**, *34*, 905.

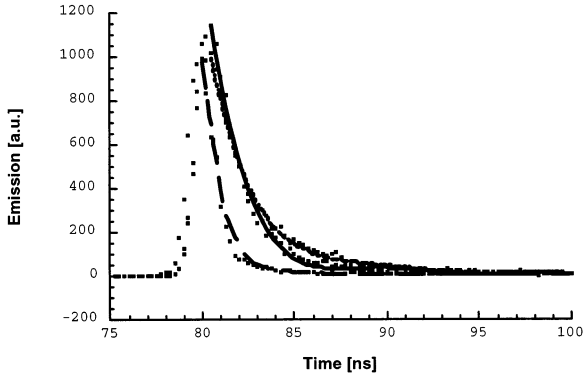

FIGURE 5. Time-resolved fluorescence decay of **1a**/**1c** (solid lines) (~1.0 × 10^{-5} M) and scatterer (dashed line). The decay curve represents the best fit to a monoexponential fluorescence decay at 640 nm (i.e., no residual ZnPc fluorescence); 337 nm excitation wavelength.

excited state is in large a spin-forbidden intersystem crossing,[18] which leads accordingly to the population of the triplet manifold, ^{3}*ZnPc (*vide supra*). For the latter transient, the following characteristics can be summarized besides the typical Soret and Q band bleaching, maxima at 500 and 785 nm.

A quantitatively similar picture was gathered for the differential absorption changes following the 355-nm excitation of **1a**−**c**, thus ensuring the selective excitation of the phthalocyanine chromophore. Again, following the conclusion of the 18-ps excitation, the singlet excited-state features are found. For example, for **1a**, maxima were found at 595, 640, 745, and 825 nm, while minima were at 617 and 675 nm. The transient spectra for **1b** and **1c** are shown in Figure 6. Relative to what we summarized for the ZnPc reference, both transient absorption and bleaching were, however, shifted toward the red region. Notably, the shifts of the features track the singlet ground-state transitions. Instead of the slow intersystem crossing in ^{1}*ZnPc, for which we determined a time constant of 3.6 ± 0.2 ns, all singlet−singlet characteristics (**1a**, 1.28 ns; **1b**, 1.54 ns; **1c**, 1.19 ns) unanimously gave rise to much faster decays. What is interesting to note is that the exact time constants are excellent matches of the fluorescence lifetimes and, more importantly, at the end of the deactivation, only the spectral features of ^{3}*ZnPc are discernible.

As far as charge separation is concerned, its implication is expected to reveal a transient maximum, which corresponds to fingerprints of $ZnPc^{\bullet+}$ and $[Ru(bpy)_3]^+$. $ZnPc^{\bullet+}$, for instance, exhibits two major transitions in the 500−960 nm region, which are located at 550 and 860 nm.[19] The changes linked to the formation of $[Ru(bpy)_3]^+$ are much weaker. Mainly, it is the bleaching of the MLCT transition at 460 nm.[20] However, no spectral evidence was found at any given delay time following the 20 ps, which could be possibly attributed to the one-electron oxidation of ZnPc or the one-electron reduction of $[Ru(bpy)_3]^{2+}$.

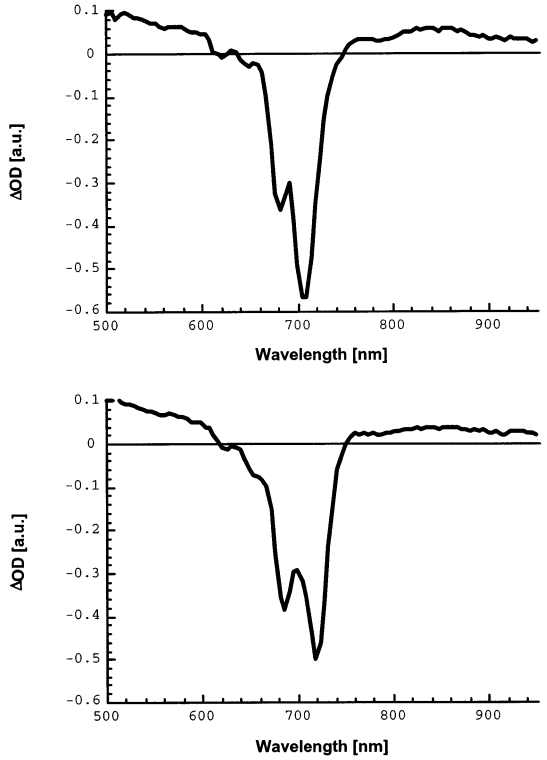

FIGURE 6. Top: Differential absorption changes recorded 50 ps after photoexcitation of **1b** in deoxygenated THF (~1.0 × 10^{-5} M). Bottom: Differential absorption changes recorded 50 ps after photoexcitation of **1c** in deoxygenated THF (~1.0 × 10^{-5} M); 355 nm excitation wavelength.

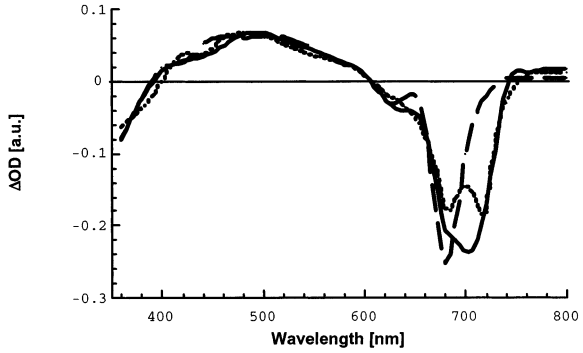

FIGURE 7. Differential absorption changes recorded 50 ns after photoexcitation of **1a** (dashed line), **1b** (solid line), and **1c** (dotted line) in deoxygenated THF (~1.0 × 10^{-5} M); 355 nm excitation wavelength.

On the nanosecond time scale, the identity of the transient species detected for **1a**−**c** is unambiguous; see Figure 7. In particular, the 500- and 785-nm maxima are clear attributes of the ^{3}*ZnPc, seen in the ZnPc reference. In addition, nearly quantitative formation, in THF and benzonitrile, with quantum yields reaching that of the **ZnPc** reference further support the conclusion that charge-transfer events (*i.e.*, endothermic and only marginally exothermic evolving from photoexcited ZnPc and $[Ru(bpy)_3]^{2+}$, respectively) play no role in photoexcited **1a**−**c**. In a strictly oxygen-free environment, the triplet excited state decayed with clean first-order kinetics, restoring the singlet ground state. Generally, triplet lifetimes of ~45 μs were deduced from the maxima in the visible (*i.e.*, 500 nm) and red (*i.e.*, 785 nm) regions.

(18) Moser, F. H.; Thomas, A. L. *The Phthalocyanines*; CRC Press: Boca Raton, FL, 1983.
(19) Guldi, D. M.; Gouloumis, A.; Vázquez, P.; Torres, T. *Chem. Commun*. **2002**, 2056.
(20) (a) D'Angelantonio, M.; Mulazzani, Q. C.; Venturi, M.; Ciano, M.; Hoffman, M. Z. *J. Phys. Chem*. **1991**, *95*, 5121. (b) Berger, R. M.; McMillin, D. R. *Inorg. Chem*. **1988**, *27*, 4245.

Conclusions

In summary, the electronic interactions in a series of multicomponent ZnPc−$Ru(bpy)_3$ systems, **1a**−**c**, have been fine tuned through the systematic variation of conjugated and/or nonconjugated connectors, linking a zinc-phthalocyanine to a ruthenium(II) tris(bipyridine) complex.

In the singlet ground state, the sharp Q band of the zinc-phthalocyanine is a particularly sensitive marker for the magnitude of interaction. It unravels broadening, red shift, and splitting with regard to the parent compounds, that is, zinc-phthalocyanine and ruthenium(II) tris(bipyridine). Even stronger are the electronic perturbations in the excited state. Following the initial excitation of either chromophore, intramolecular electronic interactions between the two subunits dominate the photophysical events. These intramolecular interactions lead, in the case of photoexcited ZnPc, to faster intersystem crossing kinetics, compared to a ZnPc reference, while photoexcited $[Ru(bpy)_3]^{2+}$ undergoes a rapid and efficient transduction of triplet excited-state energy to the Pc.

Experimental Section

General. The mass spectra (LSIMS and MALDI-TOF) were determined using *m*-NBA and dithranol, respectively, as matrices. Picosecond laser flash photolysis experiments were carried out with 355-nm laser pulses from a mode-locked (pulse width 18 ps, 2−3 mJ/pulse). Nanosecond laser flash photolysis was performed with laser pulses (355 nm, 20-ns pulse width). For all photophysical experiments, an error of 10% must be considered. Fluorescence lifetimes were measured with 337-nm laser pulses from a nitrogen laser fiber coupled to a lens-based T-formal sample compartment equipped with a stroboscopic detector. The experiments were performed at room temperature. Each spectrum was an average of at least five individual scans, and the appropriate corrections were applied.

5-[(*E*)-2-(3,4-Dicyanophenyl)ethenyl]-2,2′-bipyridine (3). A mixture of K_2CO_3 (267 mg, 1.93 mmol), 3,4-dicyanobenzylphosphonate[6b] (330 mg, 1.17 mmol), water (0.5 mL), and 5-formyl-2,2′-bipyridine[9] (220 mg, 1.17 mmol) was stirred at 100 °C for 12 h. The reaction mixture was quenched in water, filtered of the resulting precipitate, and washed repeatedly with water, affording **3** as a yellow solid (260 mg, 72%). Mp: 220 °C. ^{1}H NMR (300 MHz, $CDCl_3$): δ 8.81 (1H, d, J = 2.1 Hz, $bpyH_6$), 8.71 (ddd, J = 4.8 Hz, J = 1.6 Hz, J = 0.8 Hz, 1H, $bpyH_{6'}$), 8.48 (d, J = 8.4 Hz, 1H, $bpyH_3$), 8.44 (ddd, J = 7.8 Hz, J = 1.2 Hz, J = 0.8 Hz, 1H, $bpyH_{3'}$), 8.22 (dd, J = 8.4 Hz, J = 2.1 Hz, 1H, $bpyH_4$), 7.95 (d, J = 1.5 Hz, arom H_2), 7.86 (dt, J = 7.8 Hz, J = 1.8 Hz, 1H, $bpyH_{4'}$), 7.84 (d, J = 8.4 Hz, 1H, arom H_5 or arom H_6), 7.81 (d, J = 8.4 Hz, 1H, arom H_5 or arom H_6), 7.35 (ddd, J = 7.8 Hz, J = 4.8 Hz, J = 1.2 Hz, 1H, $bpyH_{5'}$), 7.34, 7.20 (2xd, J = 16.5 Hz, 2H, H-olefinic). ^{13}C NMR (75 MHz, $CDCl_3$): δ 159.7, 159.5, 149.1, 148,3, 142.6, 136.9, 133.8, 133.6, 131.0, 130.8, 130.1, 126.2, 124.5, 123.7, 121.0, 120.9, 115.8, 113.4. FTIR (KBr): 2231, 1586, 1459, 960, 797, 753 cm^{-1}. MS (EI$^+$) *m*/*z* (%): 308 (100, [M$^+$]). Anal. Calcd for $C_{20}H_{12}N_4 \cdot H_2O$: C, 73.61; H, 4.32; N, 17.17. Found: C, 73.67; H, 4.14; N, 17.52.

2-Aminotri-*tert*-butylphthalocyaninatozinc(II) (4). A mixture of 4-*tert*-butylphthalonitrile (552 mg, 3 mmol) and 4-aminophthalonitrile (143 mg, 1 mmol) was refluxed in DMAE (2 mL) under argon for 12 h in the presence of $ZnCl_2$ (1 mmol). After the solution cooled, the crude product was washed by centrifugation with water/methanol (10:1) and dried under vacuum. The compound was purified by column chromatography (silica gel, toluene/methanol 25:1 v/v) to yield **4** as a green solid (76 mg, 10%). Mp > 250 °C. FTIR (KBr): 3376, 2955, 1614, 1489, 1330 cm^{-1}. UV−visible in chloroform, λ_{max} (log ϵ): 682 (5.01), 617 (4.24), 351 nm (4.71). MS (LSIMS, *m*-NBA) *m*/*z* (%): 760 (100, [M + H$^+$]). Anal. Calcd for $C_{44}H_{41}N_9Zn \cdot 2H_2O$: C, 66.29; H, 5.69; N, 15.81. Found: C, 66.47; H, 5.38; N, 15.93.

(*E*)-2-(2,2′-Bipyridin-5-yl)ethenyltri-*tert*-butylphthalocyaninatozinc(II) (2a). A mixture of 4-*tert*-butylphthalonitrile (112 mg, 0.60 mmol), 5-[(*E*)-2-(3,4-dicyanophenyl)-ethenyl]-2,2′-bipyridine (**3**) (64 mg, 0.20 mmol), and $ZnCl_2$ (28 mg, 0.20 mmol) was refluxed in DMAE (2 mL) under argon for 10 h. The solvent was evaporated, and the crude product obtained was purified by chromatography (Al_2O_3 10%, tetrahydrofurane/*n*-hexane 1:3 v/v) to yield **2a** as a green solid (40 mg, 21%). Mp > 250 °C. FTIR (KBr): 2959, 2922, 2852, 1715, 1661, 1260, 1089, 1024, 801 cm^{-1}. UV−vis in tetrahydrofurane, λ_{max} (log ϵ): 688 (5.28), 677 (5.23), 613 (4.52), 352 (5.00), 225 nm (4.68). MS (LSIMS, *m*-NBA) *m*/*z* (%): 925 (100, [M + H$^+$]). Anal. Calcd for $C_{56}H_{48}N_{10}Zn \cdot H_2O$: C, 71.22; H, 5.12; N, 14.83. Found: C, 71.14; H, 5.23; N, 14.92.

(2,2′-Bipyridin-5-yl)carboxamidotri-*tert*-butylphthalocyaninatozinc(II) (2b). A solution of aminotri-*tert*-butylphthalocyaninatozinc(II) (**4**) (82 mg, 0.108 mmol) and 5-chlorocarbonyl-2,2′-bipyridine[10] (108 mg, 0.54 mmol) was stirred in *N*,*N*-dimethylacetamide (6 mL) in the presence of a catalytic amount of triethylamine. The mixture was heated at 80 °C under argon for 48 h. The solvent was removed under reduced pressure, and the residue was purified by column chromatography (silica gel, *n*-hexane/dioxane 2:1 v/v) to give 40 mg (40%) of **2b** as a blue solid. Mp > 250 °C. FTIR (KBr): 2956, 2923, 1639, 1633, 1614, 1089, 1046 cm^{-1}. UV−vis in tetrahydrofurane, λ_{max} (log ϵ): 676 (5.30), 611 (4.53), 350 (4.86), 289 (4.60), 212 nm (4.93). MS (LSIMS, *m*-NBA) *m*/*z* (%): 942 (100, [M + H$^+$]). Anal. Calcd for $C_{55}H_{47}N_{11}OZn \cdot 2H_2O$: C, 67.45; H, 4.84; N, 15.73. Found: C, 67.29; H, 5.08; N, 15.90.

(2,2′-Bipyridin-5-yl)ethynyl]-tri-*tert*-butylphthalocyaninatozinc(II) (2c). A mixture of tri-*tert*-butylethynylphthalocyaninatozinc(II) (**5**) (106 mg, 0.140 mmol), 5-bromo-2,2′-bipyridine[12] (48 mg, 0.20 mmol), and $Pd(PPh_3)_4$ (10%) was stirred at 90 °C in freshly distilled and deaerated diisopropylamine under argon for 36 h. The solvent was removed under reduced pressure, and the residue was purified by column chromatography (silica gel, chloroform/ethanol 40:1 v/v) to afford **2c** as a green solid (34 mg, 25%). Mp > 250 °C. FTIR (KBr): 2953, 2925, 2230, 1613, 1487, 1456, 1089, 1046, 746 cm^{-1}. UV−vis in tetrahydrofurane, λ_{max} (log ϵ): 687 (5.15), 671 (5.06), 633 (4.35), 610 (sh), 352 nm (4.89). MS (LSIMS, *m*-NBA) *m*/*z* (%): 923 (100, [M + H$^+$]). Anal. Calcd for $C_{56}H_{46}N_{10}Zn \cdot 2H_2O$: C, 70.03; H, 4.83; N, 14.58. Found: C, 69.91; H, 5.11; N, 14.70.

Synthesis of Ruthenium Complexes 1a−c. General Procedure. A mixture of the corresponding phthalocyaninatozinc(II) (**2a**−**c**) (0.022 mmol) and $Ru(bpy)_2Cl_2 \cdot 2H_2O$ (0.033 mmol) was dissolved in 5 mL of dry ethanol (distilled over CaO) and refluxed under argon for 24 h. After the mixture cooled, the solvent was evaporated and the remaining metal complex was taken up in hot water, filtered, and dried under reduced pressure. The solid was dissolved in a small amount of acetone, and a saturated NH_4PF_6 aqueous solution was added dropwise. The green solid was collected, washed with water−acetone (1:1), and dried under reduced pressure.

1a. Green solid (20 mg, 71%). Mp > 250 °C. FTIR (KBr): 2955, 1973, 1628, 1464, 1089, 842 cm^{-1}. UV−vis in tetrahydrofurane, λ_{max} (log ϵ): 697 (4.94), 674 (4.93), 645, 614, 355 (4.79), 289 (4.79), 211 nm (5.03). MS (MALDI-TOF, dithranol) *m*/*z* (%): 1489−1480 (100, [M − PF_6]$^+$), 1344−1335 (80, [M − 2PF_6]$^+$). Anal. Calcd for $C_{76}H_{64}N_{14}P_2F_{12}RuZn \cdot H_2O$: C, 55.40; H, 4.04; N, 11.90. Found: C, 55.21; H, 4.12; N, 11.98.

1b. Green solid (24 mg, 66%). Mp > 250 °C. FTIR (KBr): 2956, 2924, 1950, 1606, 1464, 1089, 843 cm^{-1}. UV−vis in tetrahydrofurane, λ_{max} (log ϵ): 677 (5.15), 611, 350 (4.78), 289 (4.86), 213 nm (4.98). MS (MALDI-TOF, dithranol) *m*/*z* (%): 1507−1498 (25, [M − PF_6]$^+$), 1361−1352 (100, [M − 2PF_6]$^+$).

Anal. Calcd for $C_{75}H_{63}N_{15}OP_2F_{12}RuZn\cdot 2H_2O$: C, 53.53; H, 4.01; N, 12.48. Found: C, 53.37; H, 4.04; N, 12.66.

1c. The compound was purified by column chromatography (alumina 10%, chloroform/ethanol, 3−20%). Green solid (14 mg, 40%). Mp > 250 °C. FTIR (KBr): 2953, 2925, 2230, 1613, 1487, 1456, 1089, 1046, 746 cm^{-1}. UV−vis in tetrahydrofurane, λ_{max} (log ϵ): 710 (4.55), 676 (4.51), 646, 623, 355 (4.42), 289 (4.45), 218 nm (4.41). MS (MALDI-TOF, dithranol) *m*/*z* (%): 1487−1478 (50, $[M - PF_6]^+$), 1342−1333 (100, $[M - 2PF_6]^+$). Anal. Calcd for $C_{76}H_{62}N_{14}P_2F_{12}RuZn\cdot 2H_2O$: C, 55.40; H, 4.04; N, 11.90. Found C, 55.65; H, 3.98; N, 11.83.

Acknowledgment. The authors are grateful for the financial support of the CICYT and Comunidad de Madrid (Spain) and the European Union through Grants BQU2002-04697, 07N/0030/2002, and HPRN-CT-2000-0127, respectively. Part of this work was supported by the Office of Basic Energy Sciences of the U.S. Department of Energy. This is contribution NDRL-4400 of the Radiation Laboratory.

Supporting Information Available: ^{1}H NMR and correlation spectroscopy C,H (HMQC) spectra of compound **3**. MS spectra of compounds **1a**, **1b**, **1c, 2a**, **2b**, **2c**, **3**, and **4**. This material is available free of charge via the Internet at http://pubs.acs.org.

JO0341968